Characterizing the Thrust Production of Partially-Submerged Flapping Propulsors

Ben Jin[1], Olivia Yin[2], Leah Mendelson[3]
Harvey Mudd College, [1]Engineering 2022 [2]CS-Math 2024 [3]Assistant Professor of Engineering

Overview

Motivation

When designing vehicles that can operate in both air and water, it is essential to consider a strategy for water exit. Current common solutions, namely propeller, jet, or combustion propulsion, can be highly disruptive to the environment around the vehicle. A bioinspired propulsive strategy may provide a less disruptive or more spatially compact solution.

Research Objective

To develop kinematic profiles for a bioinspired propulsor that maximize cumulative thrust generation or efficiency while translating across the water's surface.

Background

Jumping archer fish can launch themselves several body lengths, starting from directly below the water's surface [1]. To generate thrust while partially-submerged, these fish vary their tail stroke kinematics throughout a jump. Both the loss of propulsive area while partially-submerged and interactions with the free surface differentiate this case from in-water swimming. This study uses a flexible flapping plate to characterize these effects and determine partially-submerged kinematic profiles that generate the thrust necessary for water exit.

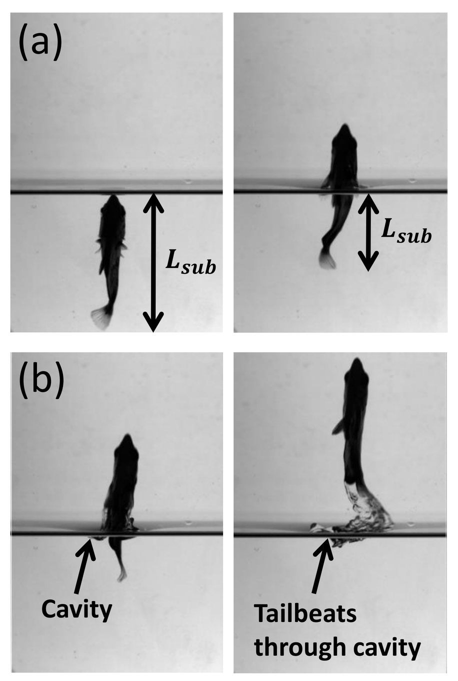

Fig. 1. Archer fish exhibiting partially-submerged propulsion (from [1]). (a) Loss of propulsive body area when partially-submerged. (b) Tailbeat interactions with the free surface.

Experiment Setup

A linkage mechanism (Fig. 2) was used to generate heaving kinematic profiles. A disk converted motor rotation into sinusoidal linear motion, shown in Fig. 3, and a servo mounted on the disk controlled the heave amplitude. Heave position was measured by a linear potentiometer and thrust forces were measured by a uniaxial load cell. Table 1 lists the parameter space for testing. Testing was conducted in two configurations, shown in Fig. 4 below. In the first configuration, also displayed in Fig. 2, the plate was secured vertically to simulate water exit. In the second configuration, the plate was secured horizontally to model in-water swimming. Each set of parameters was tested over 5 runs of 10 peak-to-peak strokes each.

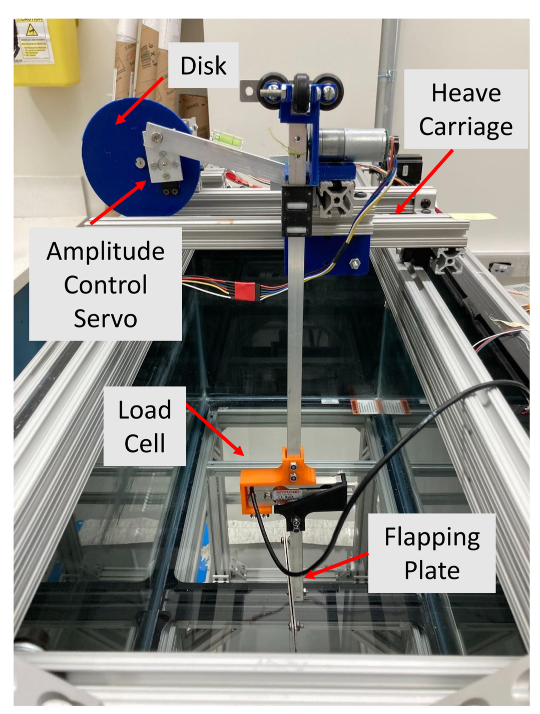

Fig. 2. Linkage mechanism, plate, and empty test tank

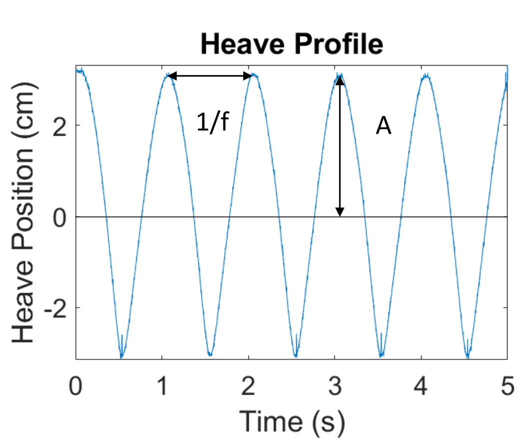

Fig. 3. Heave profile

Parameter	Variable	Values
Amplitude (cm)	A	1, 2, 3
Frequency (hz)	f	1, 2
Thickness (in)	δ	1/16", 1/32"
Stiffness (Nm^2)	EI	4.58E-3, 5.72E-4
Fraction Submerged	L_{sub}/L	1, ¾, ½, ¼

Table 1. Parameter space, stiffness calculated using $EI = \frac{Eb\delta^3}{12(1-\nu^2)}$ [2]

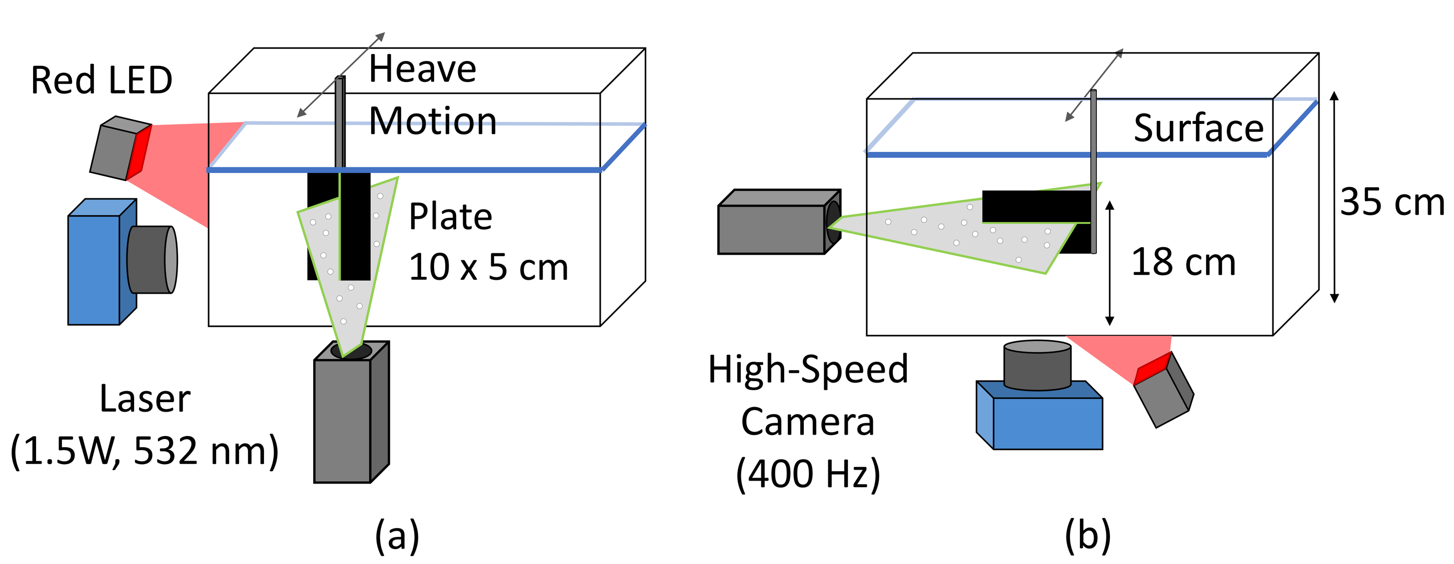

Fig. 4. PIV setup for (a) water exit and (b) in-water testing

Thrust Results

Stroke- and run-averaged thrust measurements were used to generate thrust coefficients. Since tests were performed in quiescent flow and the plate was not towed while flapping, the freestream velocity was zero. Therefore, a characteristic flapping velocity of the plate [3], in this case the heave velocity, is used to normalize thrusts (Eq. 1). In Eq. 1, T is stroke-averaged thrust force, ρ_f is fluid density, f is frequency, A is amplitude measured from centerline to peak, and b and L_{sub} are span and submerged length. While each of the plates tested had the same span and length, they were not all fully submerged, so a scaled thrust coefficient was constructed using submerged length instead of total length. Fig. 5 shows thrust coefficients generated using Eq. 1. Fig. 6 displays the stroke-averaged unscaled net thrust data.

$$C_{T,sub} = \frac{T}{2\rho_f (fA)^2 b L_{sub}} \qquad \text{Eq. 1}$$

Fig. 6 indicates that the highest net thrusts were generated by the most energetic cases, specifically the 1/16", 3cm, and 2hz cases. However, total thrust generated quickly decreased as the fraction submerged decreased, indicating diminishing returns. Despite this, thrust coefficients are still relatively high for partially submerged plates, especially for the 1/16" thickness, indicating that these low thrust cases are comparably efficient. Coefficients decrease with submerged length for the 1/32" thickness, indicating that lower flexibility plates perform better partially submerged.

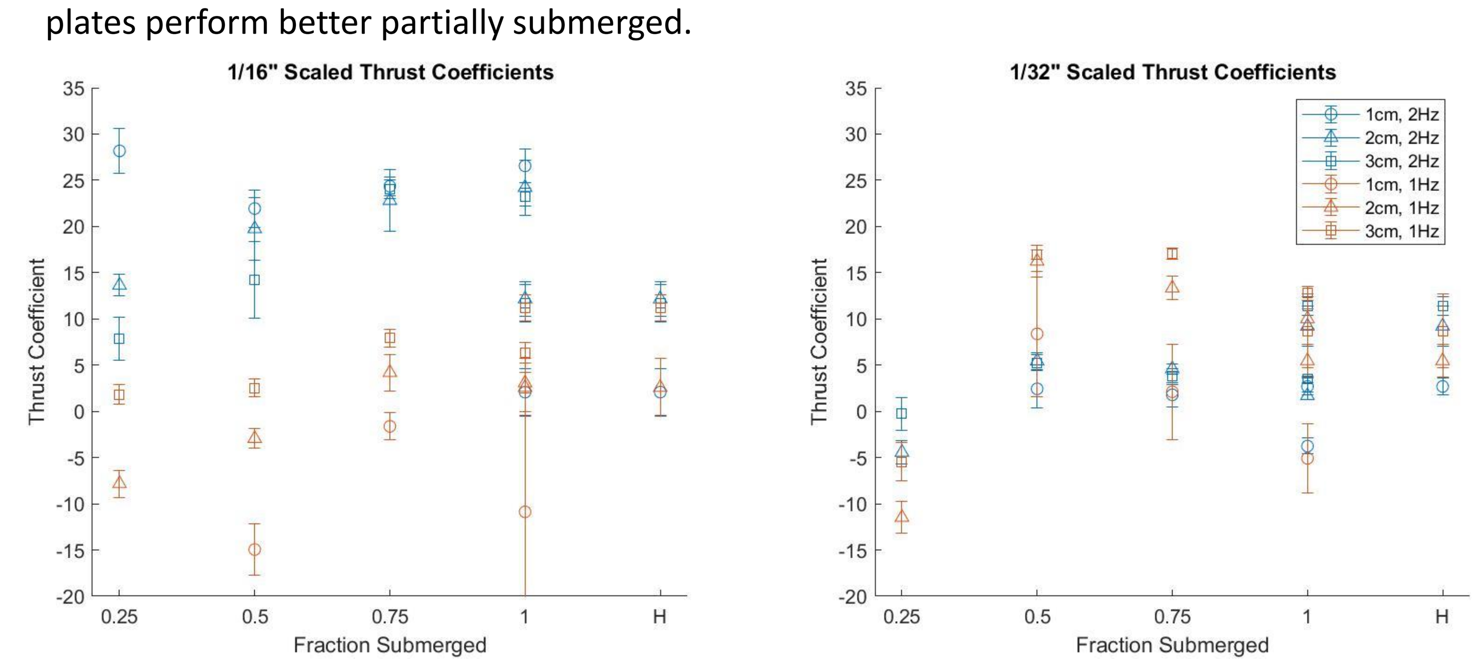

Fig. 5. Thrust coefficients scaled by submerged length. Cases that produced a thrust coefficient below -20 are not shown. Data marked H are from the horizontal in-water case.

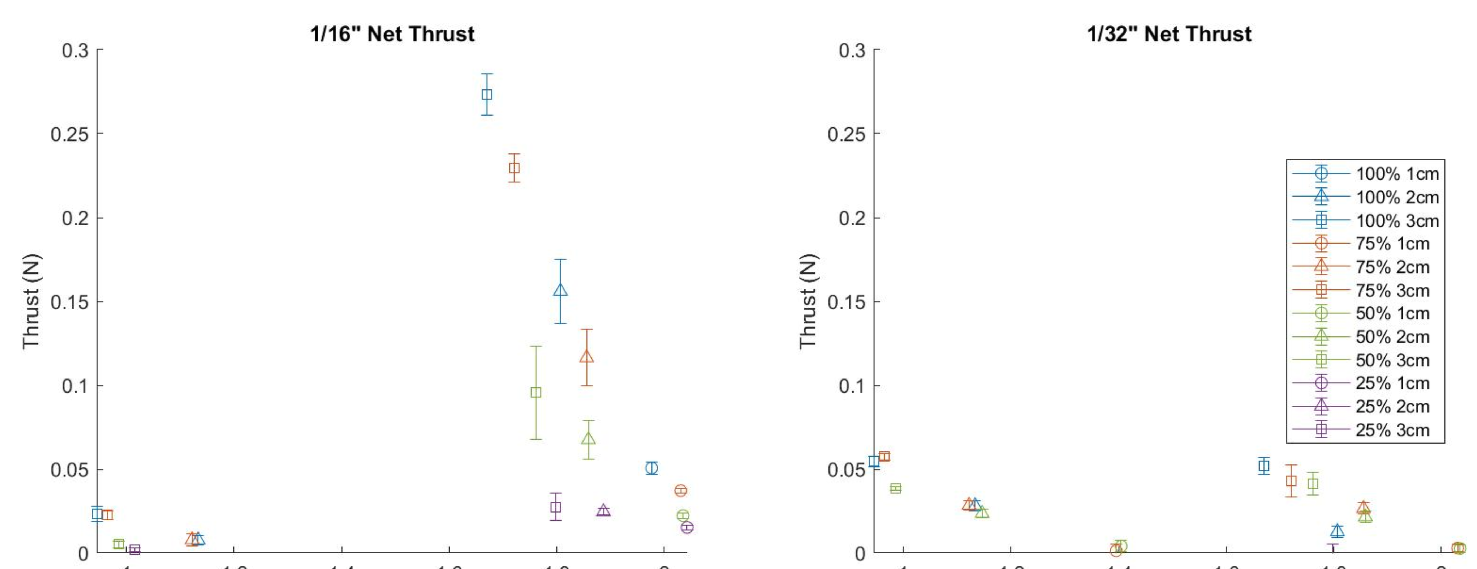

Fig. 6. Net thrust generated per stroke for the different parameters. Negative net thrusts are not included.

Particle Image Velocimetry

To compare wake structures across the parameter space, Particle Image Velocimetry (PIV) was performed for both plate configurations (Fig. 4). Reflective markers were placed along the edge of the plate to track plate bending [4] and produce masks for PIV processing [5]. To differentiate between marker points and particles, a red LED light shone onto the edge of the flexible plate (in contrast to the green laser light sheet). Red and green color channel isolation (Fig. 7) allowed for independent processing of particle and plate motion.

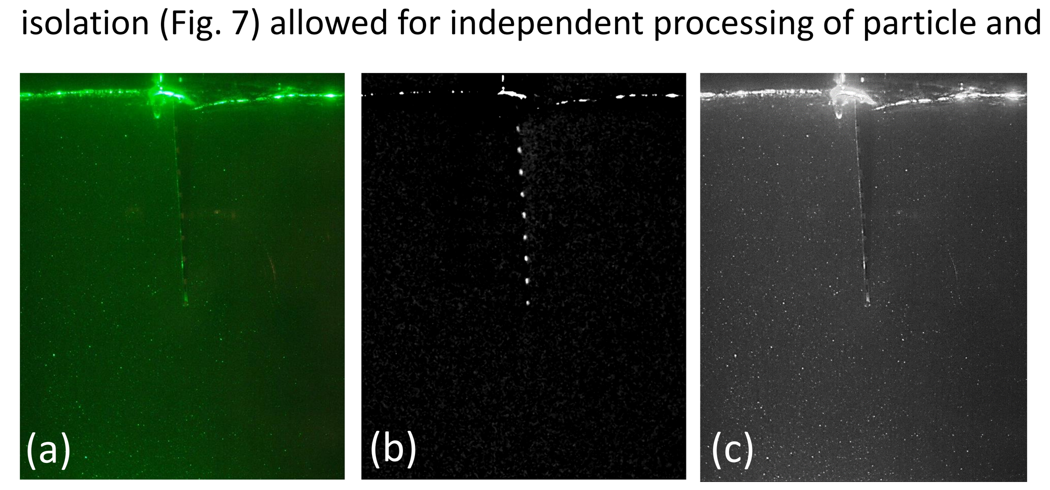

Fig. 7. Color channel isolation for plate edge tracking and PIV. (a) Original image. (b) Red channel (median-filtered and contrast enhanced). (c) Green channel (contrast enhanced).

Wake Results

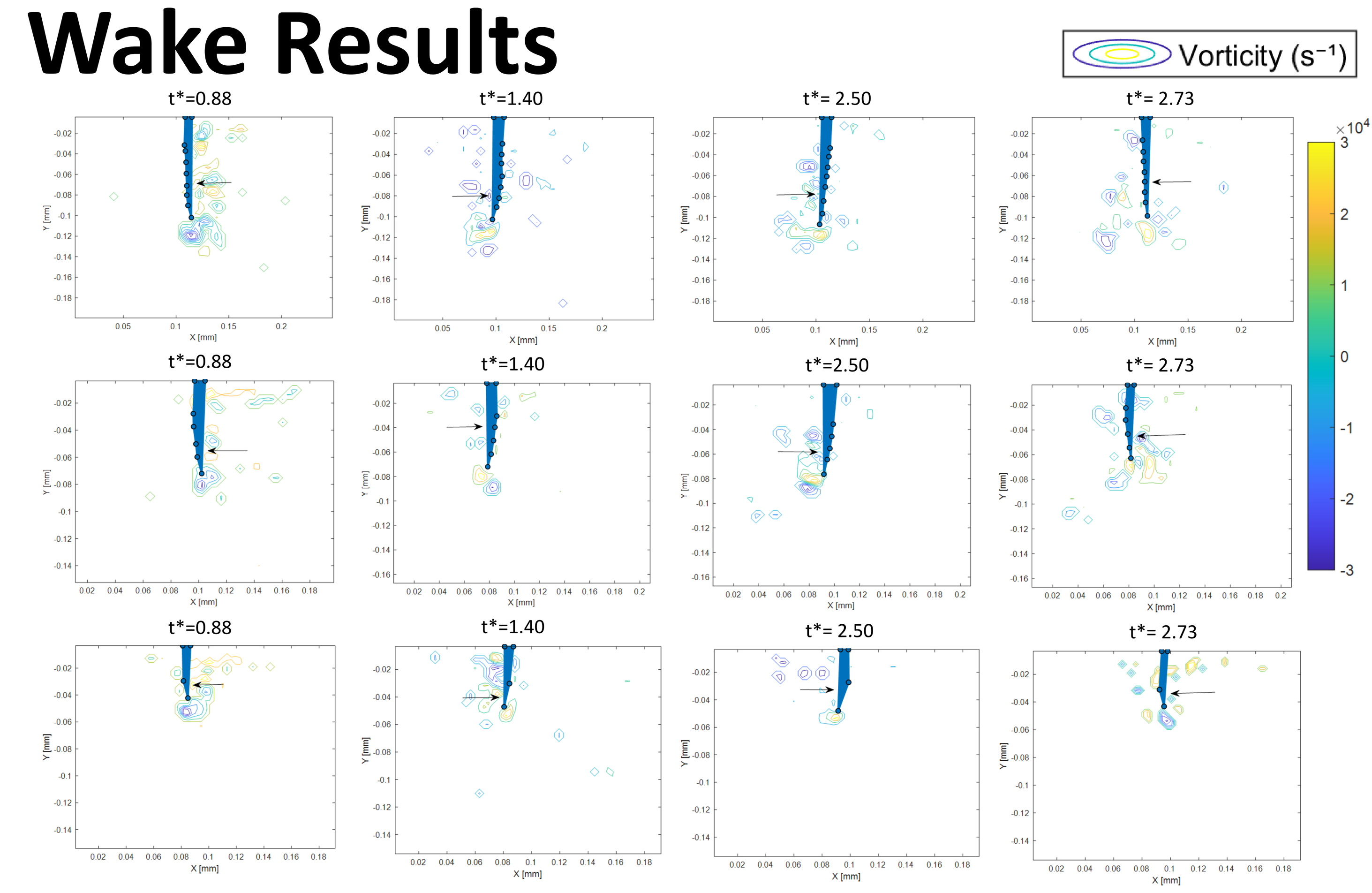

Fig 8. Wake vortices produced by the 1/16" plate for 1 cm, 2 hz flapping at $L_{sub} = L$ (top), $L_{sub} = 0.75L$ (middle), and $L_{sub} = 0.5L$ (bottom) during multiple propulsive strokes. Arrows indicate the direction of trailing edge motion. Time t* is measured from the onset of propulsive strokes and non-dimensionalized by the stroke period (0.5 s).

The wake produced by the set of parameters with the highest thrust coefficient was analyzed over two peak-to-peak propulsive strokes at varying submerged lengths (Fig. 8). Qualitatively, the same vortex shedding patterns are exhibited by the 1L and 0.75L submerged lengths. The 0.5L submerged length case shed one fewer vortex at t* = 1.40 and t* = 2.50. This change suggests that some of the hydrodynamic effects of being partially submerged are not prominent until a considerable fraction of the plate is out of the water. The wake of the fully submerged model exhibits larger and stronger vortices than the 0.75L case. This is potentially due to reduced vortex growth along the plate length and less deflection of the trailing edge when the leading 25% of the model is out of the water.

Conclusions

- Thrust can be produced, even at low submerged lengths (0.25L), by a flexible partially-submerged flapping plate actuated by heave kinematics.
- For the parameter space tested, stiffer models yield higher net thrusts and thrust coefficients while partially-submerged. The highest thrust cases do not always correspond to the highest thrust coefficients.
- Thrust variation with submerged length depends on more parameters than just submerged area, but the free surface does not significantly reduce thrust coefficients.
- Changes in wake patterns with submerged length are not prominent until a substantial fraction of the model is out of the water.

Future Work

- Utilize a multi-axis load cell to record lateral forces and evaluate efficiency
- Implement pure pitching kinematics and combined pitching and heaving kinematics
- Characterize wake variations with submerged length for a wider set of flapping parameters and stiffnesses
- Generate and test an idealized kinematic profile for flapping during towed water exit using performance data from the quiescent flapping cases

References/Acknowledgements

[1] Shih, Mendelson, Techet (2017) *J. Exp. Bio.*
[2] Quinn, Lauder, Smits (2014) *J. Fluid Mech.*
[3] Deshpande & Vishwasrao (2021) *J. Fluid Mech.*
[4] Hedrick (2008) *Bioinsp. Biomim.*
[5] Thielicke & Stamhuis (2014), *J. Open Source Softw.*

We acknowledge support from the HMC Norman F. Sprague III, M.D. Experiential Learning Fund and the Joseph Stanley Leeds Foundation Student Conference Grant. We also thank the following members of the Flow Imaging Lab at Mudd: Tian Dong, Jimmy Fernandez, Ethan Greenberg, Wing-Yee Law, Derek Li, Chris Paniagua, Louise Smith, and the following HMC staff members: Kim Neal, Drew Price, Sydney Torrey.